Engineering spin propagation across a hybrid organic-inorganic interface with a polar layer

L. Schulz[1], L. Nuccio[2], M. Willis[2], P. Desai[2], P. Shakya[2], T. Kreouzis[2], V. K. Malik[1], C. Bernhard[1], F. L. Pratt[3], N. A. Morley[4], A. Suter[5], G. J. Nieuwenhuys[5], T. Prokscha[5], E. Morenzoni[5], W. P. Gillin[2], A. J. Drew[1,2]

[1] *Department of Physics and Fribourg Center for Nanomaterials, University of Fribourg, Chemin du Musée 3, CH-1700 Fribourg, Switzerland*

[2] *Queen Mary University of London, Department of Physics, Mile End Road, London, E1 4NS, UK*

[3] *ISIS Pulsed Neutron and Muon Source, Rutherford Appleton Laboratory, Chilton, Didcot, OX11 0QX, UK*

[4] *Department of Materials Science and Engineering, University of Sheffield, Mappin Street, Sheffield, S1 3JD, UK*

[5] *Laboratory for Muon-Spin Spectroscopy, Paul Scherrer Institute, CH-5232 Villigen PSI, Switzerland*

Spintronics has shown a remarkable and rapid development, for example from the initial discovery of giant magnetoresistance in spin valves [1] to their ubiquity in hard disk read heads in a relatively short time. However, the ability to fully harness electron spin as another degree of freedom in semiconductor devices has been slower to take off. One future avenue that may expand the spintronic technology base is to take advantage of the flexibility intrinsic to organic semiconductors (OSC), where it is possible to engineer and control their electronic

properties and tailor them to obtain new device concepts [2]. Here we show that we can control the spin polarisation of extracted charge carriers from an OSC by the inclusion of a thin interfacial layer of polar material. The electric dipole moment brought about by this layer shifts the OSC highest occupied molecular orbital (HOMO) with respect to the Fermi energy of the ferromagnetic contact. This approach allows us full control of the spin band appropriate for charge carrier extraction, opening up new spintronic device concepts for future exploitation.

The development and understanding of new hybrid organic-inorganic interfaces will enable considerable progress in organic spintronics for technological purposes, including processing elements, sensors, memories, and conceptually different future applications. In addition to the "standard" spintronic applications, newly developed interfaces could bring spintronic effects to the field of organic light emitting diodes (OLED), as well as in the fast progressing field of organic field effect transistors (OFET). For example, the injection of carriers with a controlled spin state could enable the amplification of either singlet or triplet exciton states [2] leading to a significant increase in the efficiency of the electroluminescence in OLEDs. While these considerations are conceptually straightforward, no efficiency amplification has yet been reported in the literature, despite several attempts [3]. The failure of those approaches was caused by the simple reason that light emission can be detected starting from an applied voltage of a few Volts, while state-of-the-art spin injection in organic materials persists to a maximum of around 1 V [4-6]. As yet, this is unexplained. Further complications arise from the fact that various reports on working devices show a wide spread of performances for apparently similar structures, highlighting the issue of reproducibility [7-9]. The poor reproducibility is mainly due to the unknown interplay between processing and spin transfer performance and there is little deterministic control of the interface properties. However, it has recently been demonstrated that the insertion of a barrier layer on top of an organic material can

increase reproducibility for aluminium tris(8-hydroxyquinoline) (Alq_3) based spin valves [10].

Despite the reproducibility issues, the potential for organic spintronic devices appears enormous, with reports of very large spin valve magnetoresistance at low temperature [11]. One clear goal, whatever the application, is to be able to select and control the injection and extraction of spins in organic materials. This in turn requires the exquisite control of the electronic and structural states at the hybrid organic-inorganic interface [12], which until recently has only been passively determined through experiments, rather than proactively and deterministically controlled. One of the key advantages of organic semiconductors is the ease with which their electronic nature can be altered, and one such way is the use of polar materials to tune the alignment between the electrode Fermi level and the OSC molecular levels [13,14]. This has recently been demonstrated by covering a TiO_2 electrode with oriented ionic molecular monolayer of amphiphilic molecules [15]. Unfortunately, the resultant energy level shift is not well understood for any organic-inorganic interface, especially when the electrode material is ferromagnetic [13].

Here we show, using the direct spectroscopic technique Low Energy Muon Spin Rotation (LE-μSR) [16,17], that the polar material LiF reverses the spin polarisation of carriers at the NiFe interface with Alq_3. LiF has the advantage that it can be vacuum deposited over large areas, using thermal evaporation. It is a standard material used to achieve a vacuum level shift of up to 1 eV in OLED devices [18,19], via the electric dipole moment which develops due to the termination of the polar material at the interfaces. In our LE-μSR experiment, two devices were measured with an active area of 16x16 mm, comprising FeCo 17nm / Alq_3 150nm / LiF 1nm / NiFe 20nm (Sample A) and FeCo 17nm / Alq_3 150nm / NiFe 20nm (Sample B). Two identical devices were grown for the electrical and magnetoresistance (MR) measurements with an active area

of 2 x 2 mm. All samples were grown sequentially, using the same conditions in the same deposition system; further details can be found in the Methods Section. A schematic diagram of the device structure of Sample A is shown in Figure 1, which also shows the muon stopping profile for the implantation energies used in our experiments. These energies were chosen to ensure that the majority of muons stop inside the organic layer. The inset of Figure 1 shows the current-voltage characteristics of the two smaller area devices.

Figure 2(a) shows the distribution of local magnetisation, P(B), in Sample A at T=10 K for four bias voltages of 0, 1.5, 6 and 150 mV, obtained from our LE-μSR experiments. Upon applying a spin polarised current through the device, small but significant changes in the distribution P(B) are observed. These changes due to the spin polarised current can more easily be observed by taking the difference of "voltage on" and "voltage off" $P_V(B)$-$P_0(B)$. This is shown in the inset of Figure 2(a), where it can be seen that the magnetisation in the sample increases as a higher spin polarised current is passed. A quantitative description of the voltage dependence of the changes in the muon lineshapes shown in Figure 2(a) can be obtained by fitting the muon's time dependent asymmetry to a skewed Lorentzian relaxation function [16], comprising a skewness parameter and peak field (corresponding to the mode of the field distribution). It has previously been shown that the skewness parameter, Δ, is a very sensitive probe of the polarisation of the injected charge carriers [16]. To understand how a change in injected spin polarisation alters Δ, we must first define spin majority holes or electrons to be those that extract to or inject from the spin majority band of the relevant ferromagnetic contact, and vice versa for the spin minority carriers. If Δ increases on the application of a spin polarised current, the muons are measuring a higher magnetic field due to the magnetisation resulting from a population imbalance of the two spin channels in favour of spin majority electrons, either by extraction of spin majority holes in the HOMO or injection of spin majority electrons in the LUMO. On the other hand, if Δ decreases, the

muons measure a lower magnetic field from the imbalance in favour of spin minority carriers.

The obtained peak field and skewness, obtained from the time domain fits, are then plotted as a function of voltage in Figures 2(b) and 2(c). The peak field that the muons experience increases as the bias voltage on the device increases and there is a noticeable enhancement of the skewness of the lineshape. All observed effects here are consistent with spin-polarised charge carriers being injected into the organic layer, with this sample showing very similar behaviour to one previously studied, which had a very similar structure also including a LiF interfacial layer [16]. However, as is evident from all of the data presented in Figure 2, the magnetisation resulting from the spin polarised current appears to saturate at higher voltages. It is interesting to note that spin injection into organic materials has so far only been demonstrated for voltages below approximately 1 V, with the largest MR observed typically at 100 mV and below [4,20,21]. Indeed, as can be seen from Figure 2(d), this very trend is observed in our devices, with the saturation voltage observed in our muon experiments corresponding well to the loss of magnetoresistance. Clearly, there is a loss of spin polarisation with increasing voltage, as the μSR lineshape skewness and peak field should scale with current if the polarisation remains unchanged, whereas the MR as plotted in Figure 2(d) should scale with polarisation and be independent of current.

Strong electrical dipoles are present at many OSC-Metal interfaces and these interfacial dipoles can significantly alter the non-interacting equilibrium energy levels [11,13,14, 22-28]. Thus far, little is experimentally known about the role of these vacuum level shifts on spin injection and extraction. Clearly, a spectroscopic study of spin propagation investigating the effect of such an energy shift is crucial for the understanding of the spin transport properties of hybrid ferromagnetic–organic devices. For this reason we performed LE-μSR measurements on a second sample – nominally

identical to the first one, other than the absence of the thin LiF layer at the cathode interface. Plotted in Figure 3(a-d) is the bias voltage dependence of the change in skewness for both samples and the corresponding magnetoresistance. Also plotted in Figure 3(c) and (d) are the voltage dependent peak field and magnetoresistance, respectively, for the sample without the LiF layer. It is immediately clear that the presence of the LiF layer *reverses* the spin polarisation in the Alq_3. Since this phenomenon is likely due to a vacuum level shift at the interface changing the relevant spin-band, we must first understand which molecular orbitals are responsible for the current in our devices before we can discuss the origin of the spin-reversal. From the IV characteristics (inset to Figure 1) it can be seen that the contacts are almost Ohmic with only a very small and symmetrical built-in potential. Given that the devices were being operated with the FeCo contact as the anode, the current in the device is due to one of the two following phenomena. Either holes are being transported in the HOMO, entering the Alq_3 from the anode and exiting at the cathode, or electrons are being transported in the LUMO, entering at the cathode and exiting at the anode. As the work function of the transition metals are very high (~4.5 eV for Fe and ~5 eV for Co and Ni) [29] the possibility of electron injection into the Alq_3 is unlikely, particularly given that the devices operate at less than 100 mV. It seems likely that the current in the device is therefore carried predominantly by holes traversing the HOMO [30].

Injection into an OSC can only occur from within a few kT of the Fermi Energy of the electrode; in the case of holes, as in our devices, there need to be unoccupied states in the FeCo anode. The spin polarisation of the injected holes is therefore determined by the spin density of states (DoS) at the Fermi Energy of the ferromagnet. In contrast, any energy below the Fermi Energy can accept a hole being extracted, provided there is a non-zero DoS in the cathode at the energy corresponding to the HOMO of the OSC. This process is schematically shown in Figure 4(a), where hole injection occurs near the Fermi Energy and extraction below it. As stated earlier, the

interface dipole introduced by LiF produces a vacuum level shift, which moves the HOMO energy relative to the Fermi Level of the metal contact. This is schematically shown in Figure 4(b) and (c), which compares spin dependent hole extraction with and without the LiF induced vacuum level shift. Since the spin dependent hole extraction probability depends on the spin polarisation in the cathode at the OSC HOMO energy, a shift in the HOMO would change the spin polarisation of extracted holes (see Figure 4) [13]. This can easily explain the data presented in Figure 3. We would like to note that it has already been suggested that changes in coupling at the interface between the OSC and ferromagnet can alter the spin polarisation of injected electrons [11].

For the device without the LiF layer (Sample B, Figure 3(c) and (d)), at the magnetic fields where the LE-μSR measurements were carried out the magnetisation of the two contacts are aligned. The change in skewness close to the cathode is negative, indicating that the total field is lowered by the spin polarised hole extraction (upper schematic plot in Figure 3(f)). This must mean that the extracted holes are spin minority, as there must be an excess of electron spins opposed to the applied field as shown in Figure 4(e), which would result in a lowering of the magnetic field observed by the muons (lower schematic plot in Figure 3(f)). Since the sample is in a high resistance state when the FM's have their magnetisation aligned, the two electrodes must inject/extract opposite spins and therefore the anode must be injecting spin majority holes (lower schematic plot, Figure 3(f)). For the device with a LiF layer (Sample A, see Figure 3(a) and (b)), the anode is unchanged and so should still be injecting spin majority holes. However, if the extraction spin band is altered at the cathode, one would expect spin majority hole extraction (see lower schematic plot, Figure 3(e)). This would lead to a spin majority electron accumulation at the cathode interface as shown in Figure 4(d), which results in an increased magnetisation (see upper schematic plot, Figure 3(e)) and consequently a positive change in skewness - as is observed in Figure 3(b). Since both electrodes would be efficiently

injecting/extracting spin majority holes, one would expect the device to be in a low resistance state when the two FM layers have aligned magnetisations, as is observed in Figure 3(a). It is worth noting that changes to the tunnelling matrix element, if this is the relevant spin transfer mechanism into the OSC, could also contribute to a different spin transfer across the interface [31,32]. This can arise if one considers the matching condition for the k-vectors of the evanescent wave in a tunnelling barrier present and the one in the FM. However, it can also lead to a bias dependent reversal of the injected spin polarisation [31], which has never been observed in OSC spinvalve structures.

These results are particularly exciting for spintronics applications as they demonstrate that the dominant spin band for charge carrier extraction can be modified through the introduction of an interfacial layer, as has already been predicted [11,13]. They also highlight the possibility for the engineering of more complex devices where spins can be manipulated. For example, for a metal sandwiched between two organic materials, it would be possible to extract spins with one polarisation from an OSC and inject the opposite spin polarisation into another OSC, and this could be switchable. If the polar layers were ferroelectrics, then it could be possible to switch the polarisation of the electric dipole moment with an electric field, thus the device could act as a spin filter or switch. Furthermore, spatially patterning alternate orientation of the polar materials may yield interference of spin polarised currents, which could be used as a spin interferometer. Clearly, it should be possible to enhance the effects observed here, by growing epitaxial or self-assembled films with a preferred ionic orientation. It would also be interesting to perform LE-μSR experiments for both positive and negative bias, at both injection and extraction electrodes. These could shed light on the unsymmetrical nature of the voltage dependent reduction in MR [5]. It is unlikely that the polarisation of extracted holes is symmetrical with positive/negative voltage as the extraction polarisation depends on the density of states at the HOMO energy of the extracting electrode. The inclusion of a LiF layer should not affect the spin polarisation of injected

holes, since these are injected within a few kT of the Fermi surface. If this study was repeated with an LSMO electrode, it would be possible to differentiate between our model and the one proposed by Barraud and co-workers [11]. Finally, we would like to note that the magnitude of the MR and muon signal is similar for both of our devices, suggesting that there is no fundamental obstacle to injecting or extracting polarised charge carriers from transition metal FM at higher voltages. In our case, we were able to access states with different polarisation via a vacuum level shift, but these may equally well be accessed by the choice of OSC or an increased bias voltage.

Methods

Samples

The devices were grown on a high-purity fused quartz substrate with an rms roughness of less than 2 nm. Alq_3 (99.995% pure) was purchased from Aldrich and purified by train-sublimation under a 10^{-6} mbar vacuum. The Ni, Co and Fe were purchased from Aldrich (>99.9% pure) and pressed into pellets in the proportions 80:20 Ni:Fe and 50:50 Fe:Co, which were subsequently thermally evaporated. High purity aluminium, purchased from Adrich, was evaporated at the edges of the sample to enable contacts to be made effectively; the contacts were well away from the centre of the beam, such that less than 2% of the beam hit the contacts [16]. The deposition of the Alq_3 and LiF layers was performed using a Kurt J. Lesker SPECTROS evaporation system under ~10^{-7} mbar. Magnetic layers were evaporated in a separate system under ~10^{-6} mbar vacuum. A calibrated oscillating quartz crystal monitor was used to determine the rate and thickness of all deposited layers. X-ray reflectivity was used to estimate the thickness of each layer and the interface roughness. The deposition rate of the Alq_3, Al and LiF was maintained at 0.2 nm/s and that of the magnetic contacts at around 0.1 nm/s. Shadow masks were used to define the device geometry.

LE-μSR

Positive muons decay to a positron, muon antineutrino and electron neutrino. The angular emission of positrons is well characterised, with the emission direction being correlated with the muon's spin at time of decay. Thus, by measuring the direction and the timing of a statistically significant number of decay positrons it is possible to follow directly the evolution of the spin of the ensemble of muons as a function of time after implantation. Muons can act as passive local magnetic microprobes, by directly measuring magnetic field distribution at the implanted site with very high sensitivity

(less than 0.1 mT). Being able to follow the evolution of the spin with time means that the local magnetic field experienced by the muon can be determined through the measurement of the Larmor precession of the muon spin, which is obtained using two positron counters mounted on opposite sides of the sample. We used a bespoke floating power supply/volt meter that could bias the sample to a high degree of accuracy (+/- 0.1 nA and +/- 0.1 μV) whilst floating the sample at +/- 10 kV. The high voltage is necessary for controlling the muon implantation energy and thus the muon stopping distribution within the device. Electrical contacts were made using spring loaded electrodes supported by PTFE blocks and the whole assembly was mounted on a high-purity Ag coated Al plate. The magnetic field was applied parallel to the layers and perpendicular to the muon's initial spin direction and momentum. The measurements proceeded by first applying a field of 100 mT to ensure that the FM layers were saturated, after which the magnetic field was reduced to 27 mT. The μSR spectra were first obtained with the current on and then with current off.

In our LE-μSR experiment, 200-300 nm of a weakly bound van der Waals cryosolid multilayer (solid-Ar / solid-N_2) was deposited on the downstream side of a cold metal substrate, which moderates a fraction of an intense surface muon beam to ~15 eV (with a similar root mean square energy spread) whilst conserving the initial full polarisation. The epithermal muons are extracted (by applying up to +20 kV to the moderator substrate), transported and focused by electrostatic elements to the sample. A trigger detector provided a muon start signal by detecting secondary electrons, released by the muons when passing through a 2 $\mu g/cm^2$ carbon foil onto a microchannel plate detector. The mean implantation energies were 4.25, 6.23 and 9.23 keV, controlled by choosing the appropriate moderator, transport and sample voltages. The muon's stopping profile can be calculated using a Monte-Carlo algorithm TRIM.SP [32]. This is shown in relation to our devices in Figure 1. By varying the muon's stopping profile, we were able to probe depth profile of the induced magnetisation due to injected spin

polarised charge carriers. Further information regarding the technique can be found in refs [16, 17, 34].

References

[1] M. N. Baibich et al., *"Giant Magnetoresistance of (001)Fe/(001)Cr Magnetic Superlattices"*, Physical Review Letters 61, 2472 – 2475 (1988).

[2] I. Bergenti et al., *"Spin polarised electrodes for organic light emitting diodes"* Organic Electronics 5, 309-314 (2004).

[3] G. Salis, S. F. Alvarado M. Tschudy, T. Brunschwiler and R. Allenspach, *"Hysteretic electroluminescence in organic light-emitting diodes for spin injection"* Physical Review B 70, 085203 (2004).

[4] Z. H. Xiong, D. Wu, Z. Vardeny and J. Shi, *"Giant magnetoresistance in organic spin-valves"* Nature 427, 821-824 (2004).

[5] V. A. Dediu, L. E. Hueso, I. Bergenti and C. Taliani, *"Spin routes in organic semiconductors"*, Nature Materials 8, 707-716 (2009).

[6] R. Lin, F. Wang, J. Rybicki, and M. Wohlgenannt and K. A. Hutchinson, *"Distinguishing between tunnelling and injection regimes of ferromagnet/organic semiconductor/ ferromagnet junctions"*, Physical Review B 81, 195214 (2010).

[7] S. B. Jiang, J. E. Pearson & S. D. Bader, *"Absence of spin transport in the organic semiconductor Alq(3)"*, Physical Review B 77, 035303 (2008).

[8] J. J. H. M. Schoonas et al., *"Magnetoresistance in Hybrid Organic Spin Valves at the Onset of Multiple-Step Tunnelling"*, Physical Review Letters 103, 146601 (2009).

[9] D. L. Sun et al., *"Giant Magnetoresistance in Organic Spin Valves"*, Physical Review Letters 104, 236602 (2010).

[10] V. Dediu et al., *"Room-temperature spintronic effects in Alq_3-based hybrid devices"* Physical Review B 78,115203 (2008).

[11] C. Barraud et al., *"Unravelling the role of the interface for spin injection into organic semiconductors"*, Nature Physics 6, 615 - 620 (2010).

[12] M. Cinchetti et al., *"Determination of spin injection and transport in a ferromagnet/organic semiconductor heterojunction by two-photon photoemission"*, Nature Materials, 8, 115-119 (2009).

[13] N. Atodiresei et al., *"Design of the Local Spin Polarization at the Organic-Ferromagnetic Interface"*, Physical Review Letters 105, 066601 (2010).

[14] I. H. Campbell et al., "*Controlling charge injection in organic electronic devices using self-assembled monolayers*" Applied Physics Letters 71, 3528-3530 (1997).

[15] H. J. Bolink et al., *"Molecular ionic junction for enhanced electronic charge transfer"*, Langmuir 25, 79-83 (2009).

[16] A. J. Drew et al., *"Direct measurement of the electronic spin diffusion length in a fully functional organic spin valve by low-energy muon spin rotation"*, Nature Materials 8, 109-114 (2009).

[17] E. Morenzoni et al, *"Generation of very slow polarized positive muons"*, Physical Review Letters 72, 2793-2796 (1994).

[18] H Ishi et al., *"Energy-level alignment at model interfaces of organic electroluminescent devices studied by UV photoemission: Trend in the deviation from the traditional way of estimating the interfacial electronic structures"*, IEEE Journal of Selected Topics in Quantum Electronics 2, 24-33 (1998).

[19] H. Shii & K. Seki K, *"Energy level alignment at organic/metal interfaces studied by UV photoemission: Breakdown of traditional assumption of a common vacuum level at the interface"* IEEE Transactions on Electron Devices 44, 1295-1301 (1997).

[20] F. J. Wang, C G Yang, Z Vardeny and X Li, *"Spin response in organic spin valves based on $La_{2/3}Sr_{1/3}MnO_3$ electrodes"*, Physical Review B 75, 245324 (2007).

[21] F. J. Wang and Z V Vardeny, *"Recent advances in organic spin-valve devices"*, Synthetic Metals 160, 210–215 (2010).

[22] S. Majumdar, H. S. Majumdar, R. Laiho & R. Osterbacka *"Comparing small molecules and polymer for future organic spin-valves"*, Journal of Alloys and Compounds. 423, 169–171 (2006).

[23] Y. Zhan, I. Bergenti, L. E. Hueso & V. Dediu *"Alignment of energy levels at the $Alq_3/La_{0.7}Sr_{0.3}MnO_3$ interface for organic spintronic devices"* Physical Review B 76, 045406 (2007).

[24] Y. Q. Zhan et al. *"Energy level alignment and chemical interaction at Alq3/Co interfaces for organic spintronic devices"* Physical Review B 78, 045208 (2008).

[25] Y. Q. Zhan et al. *"The role of aluminium oxide buffer layer in organic spin-valves performance"* Applied Physics Letters 94, 053301 (2009).

[26] M. V. Tiba, W. J. M. de Jonge, B. Koopmans & H. T. Jonkman *"Morphology and electronic properties of the pentacene on cobalt interface"* Journal of Applied Physics 100, 093707 (2006).

[27] M. Popinciuc, H. T. Jonkman & B. J. van Wees *"Energy level alignment symmetry at Co/pentacene/Co interfaces"* Journal of Applied Physics 100, 093714 (2006).

[28] M. Grobosch, K. Dorr, R. B. Gangineni & M. Knupfer *"Energy level alignment and injection barriers at spin injection contacts between $La_{0.7}Sr_{0.3}MnO_3$ and organic semiconductors"* Applied Physics Letters 92, 023302 (2008).

[29] "Handbook of Physics and Chemistry 90th edition", D. R. Lide (ed.).

[30] N. A. Morley et al., *"Room temperature organic spintronics"*, Journal of Applied Physics 103, 07F306 (2008).

[31] D. L. Smith and P. P. Ruden, "*Spin-polarized tunnelling through potential barriers at ferromagnetic metal/semiconductor Schottky contacts*", Physical Review B 78, 125202 (2008).

[32] S. O. Valenzuela, D. J. Monsma, C. M. Marcus, V. Narayanamurti, and M. Tinkham, *"Spin Polarized Tunneling at Finite Bias"*, Physical Review Letters 94, 196601 (2005).

[33] E. Morenzoni, et al., *"Implantation studies of keV positive muons in thin metallic layers"*, Nuclear Instrumentation Methods B 192, 254–266 (2002).

[34] T. Prokscha et al, *"The new μE4 beam at PSI: a hybrid-type large acceptance channel for the generation of a high intensity surface-muon beam"*, Nuclear Instruments and Methods A 595 317-331 (2008).

Author Information

Correspondence to WPG (W.Gillin@qmul.ac.uk) and AJD (A.J.Drew@qmul.ac.uk).

Author Information

A.J.D. was responsible for project planning and concept. L.S., L.N., M.W., V.K.M, C.B., F.L.P., N.A.M., A.S., G.J.N., T.P., E.M. and A.J.D. were responsible for the experimental measurements. L.S., L.N., W.P.G. and A.J.D were responsible for the analysis and interpretation of results. P.D., P.S., T.K., W.P.G. and A.J.D. were responsible for the sample growth and characterization.

Acknowledgements

AJD acknowledges financial support from the Royal Society, Leverhulme Trust and the EPSRC (grant EP/G054568/1), CB from the SNF (grant 200020-119784 and 200020-129484) and the NCCR program MaNEP and NAM from the British Council. This experimental work was partly performed at the Swiss Muon Source SμS.

Figure 1: **A schematic diagram of the device structure.** The muon's stopping profile is plotted for Sample A, calculated with a Monte Carlo algorithm (see Methods). A similar profile is obtained in Sample B. Inset: The IV characteristics measured on the two small area devices – with LiF and without LiF (Sample A and B respectively).

Figure 2: **Spin polarised charge carriers are present in the OSC, close to the top NiFe interface.** (a): Probability distribution of magnetic field inside the device with LiF (Sample A) at several different voltages. Inset: the difference between the data with and without an applied voltage, where a clear increase in the difference signal amplitude is observed at higher voltages. (b): The change in lineshape skewness and (c): peak field clearly saturates at higher voltages. A clear reversal in the voltage dependence of the peak field is observed in (c) when the LiF layer is omitted. (d): The magnetoresistance for devices with and without LiF. The reduction of magnetoresistance occurs at similar voltages to the saturation of the LE-μSR data shown in (b) and (c). Muon measurements were taken at a temperature of 10K and at an energy of 6.23 keV. The MR was taken at 20K. In plots 1b-c, error bars represent one standard deviation, calculated from the Poissonian statistics of the muon data. For (d), the error bars represent an estimate of the scatter present in the MR data. In (b) and (c), the lines are guides to the eye.

Figure 3: **A comparison of the device magnetoresistance and spin polarisation close to the top interface.** (a):The magnetoresistance and (b) the change in μSR lineshape skewness for Sample A, with the LiF layer. (c): The magnetoresistance and (d): the change in μSR lineshape skewness for Sample B, without the LiF layer. Muon measurements were taken at a temperature of 10K, with the MR measurements taken at a bias of 20mV and at 20K. As can be seen from (a)-(d), there is a clear reversal of spin polarisation as a result of the presence of the LiF layer. This is due a change of extracted spin polarisation brought about by a vacuum level shift due to the electric dipole moment induced by the LiF. (e): For spin majority hole extraction there is an increase in magnetisation close to the interface. (f): For spin minority hole extraction, there is a decrease in magnetisation close to the interface. In (e) and (f), the red shaded area and spins correspond to hole injection whereas the blue corresponds to hole extraction. In (b) and (d), error bars represent one standard deviation and the lines are guides to the eye.

Figure 4: **Schematic diagram of hole transport in OSC and how a vacuum level shift leads to a change of extracted spin polarisation.** (a): Hole injection occurs close to the Fermi Level, since there must be vacant states in the FM in order for injection to occur. Conversely, hole extraction can take place anywhere below the Fermi Level. (b, d): As holes are extracted, the probability of one particular spin state dominating the extraction is related to the spin density of states at the extraction energy. For the case of the device with LiF where there is a vacuum level shift δ, this results in electron majority spin accumulation, as spin majority holes are extracted more efficiently. (c, e): For the device without the LiF layer, the vacuum level shift is not present. This

results in a probability of extraction such that the most probable extracted hole polarisation is spin minority, leading to an accumulation of spin minority electrons close to the interface.

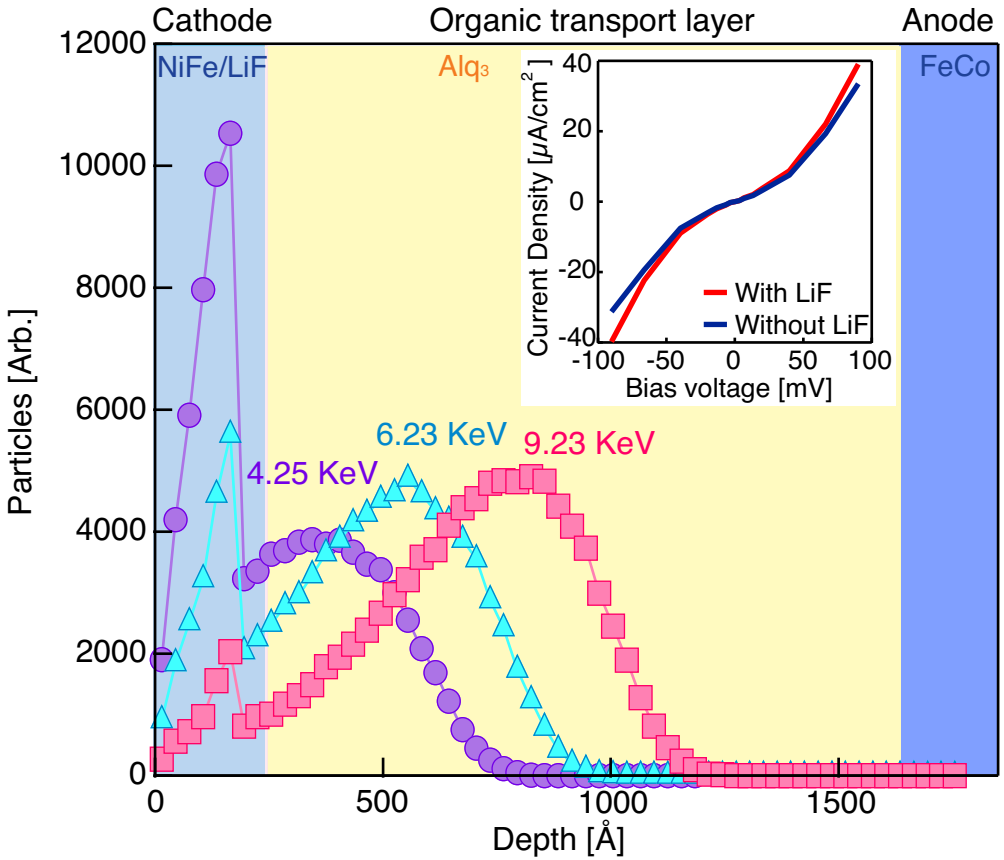
Cathode
Organic transport layer
Anode
NiFe/LiF
Alq3
FeCo
Particles [Arb.]
Depth [Å]
4.25 KeV
6.23 KeV
9.23 KeV
Current Density [μA/cm²]
Bias voltage [mV]
With LiF
Without LiF

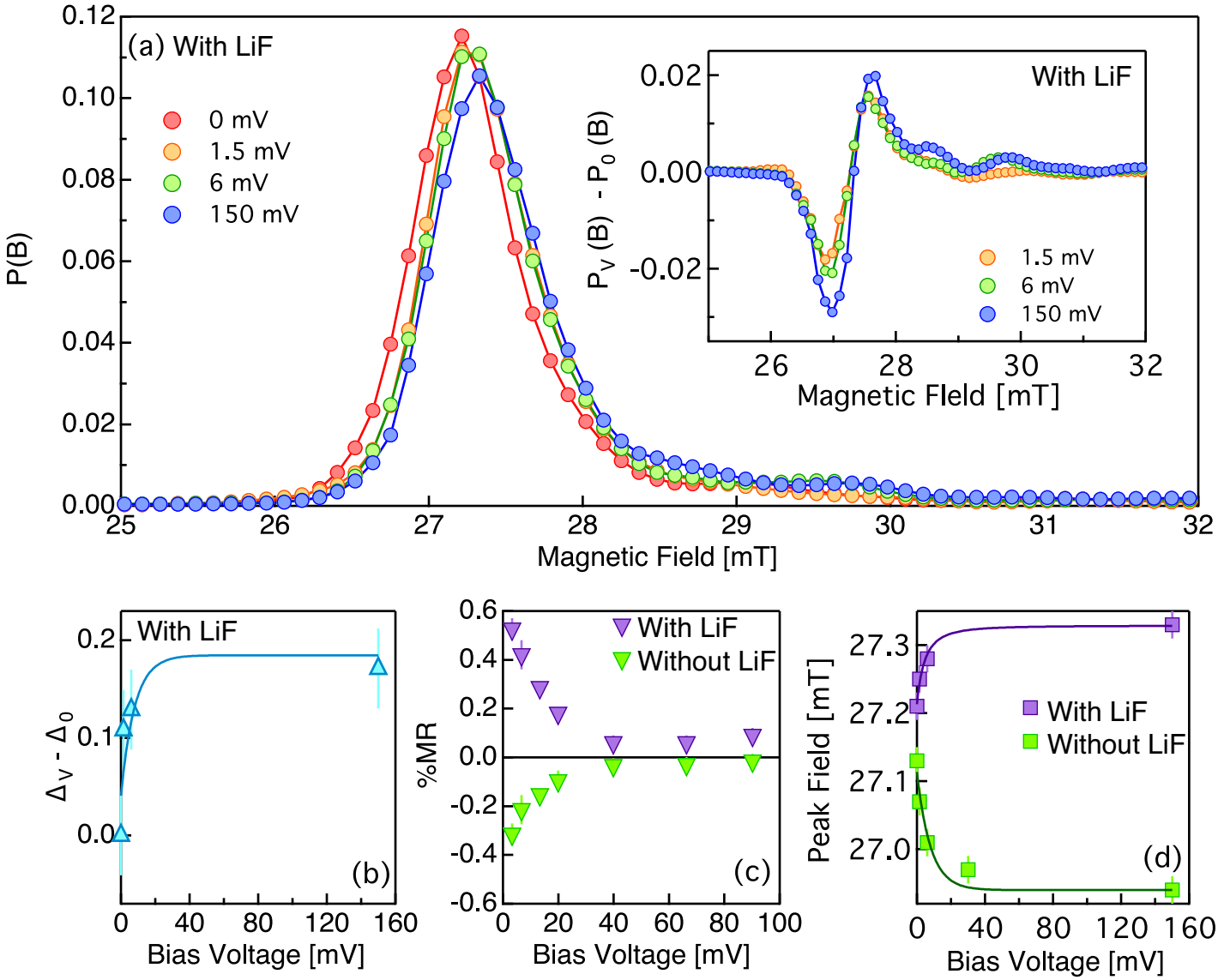
(a) With LiF
0 mV
1.5 mV
6 mV
150 mV
P(B)
Magnetic Field [mT]
With LiF
$P_V(B) - P_0(B)$
1.5 mV
6 mV
150 mV
Magnetic Field [mT]
With LiF
$\Delta_V - \Delta_0$
(b)
Bias Voltage [mV]
With LiF
Without LiF
%MR
(c)
Bias Voltage [mV]
With LiF
Without LiF
Peak Field [mT]
(d)
Bias Voltage [mV]

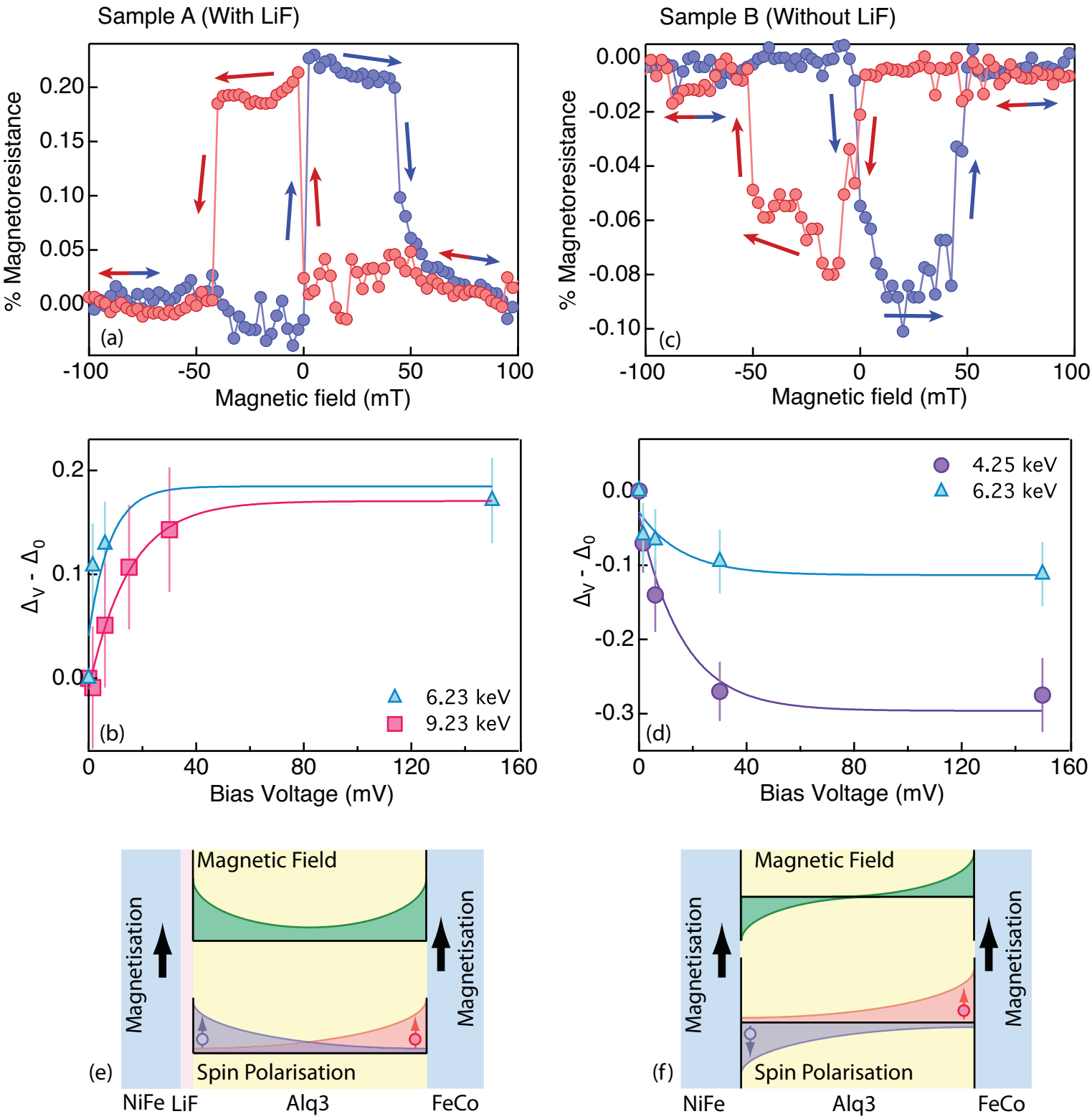
Sample A (With LiF)
Sample B (Without LiF)
% Magnetoresistance
Magnetic field (mT)
(a)
(c)
(b)
(d)
$\Delta_V - \Delta_0$
Bias Voltage (mV)
6.23 keV
9.23 keV
4.25 keV
6.23 keV
Magnetic Field
Spin Polarisation
Magnetisation
NiFe
LiF
Alq3
FeCo
(e)
(f)

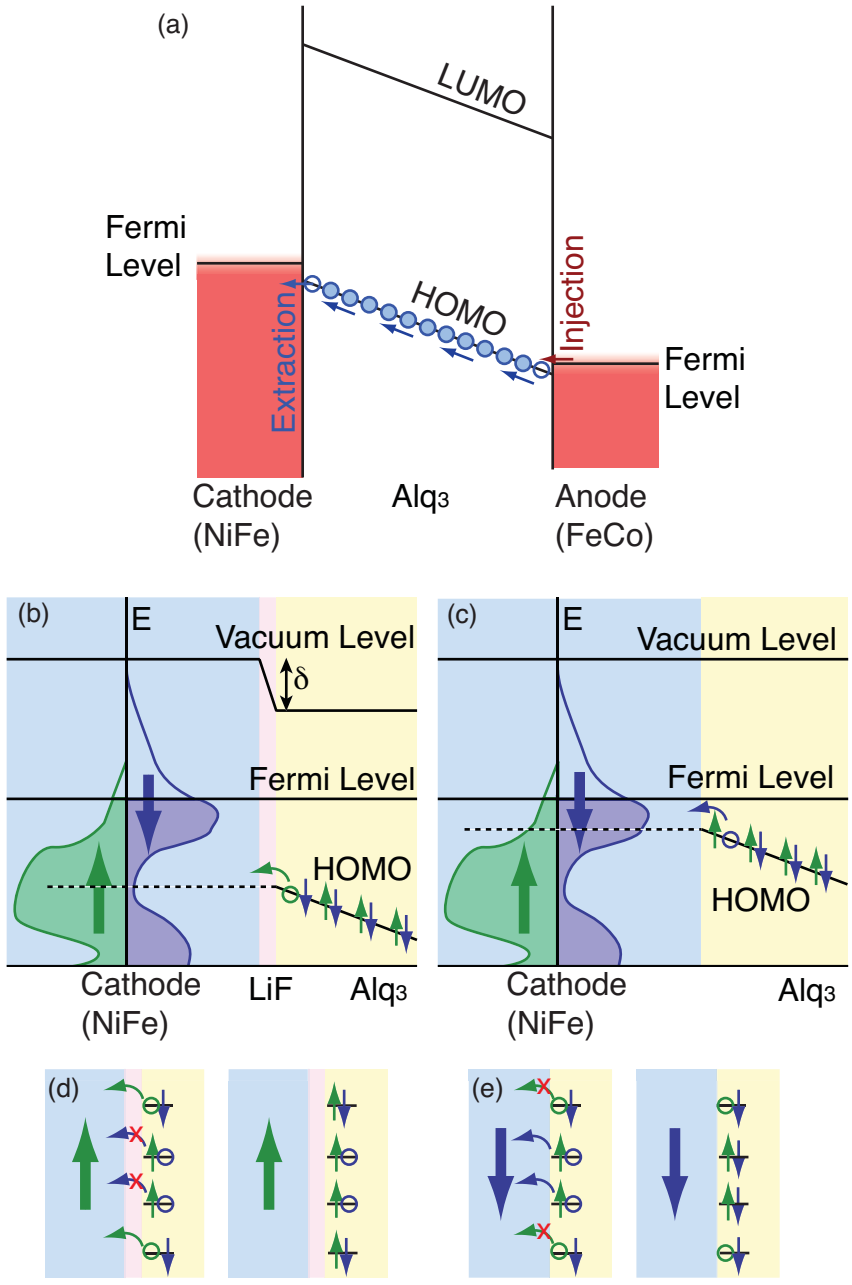
(a)
LUMO
Fermi
Level
HOMO
Extraction
Injection
Fermi
Level
Cathode
(NiFe)
Alq3
Anode
(FeCo)
(b)
E
Vacuum Level
δ
Fermi Level
HOMO
Cathode
(NiFe)
LiF
Alq3
(c)
E
Vacuum Level
Fermi Level
HOMO
Cathode
(NiFe)
Alq3
(d)
(e)